PART IB ENGINEERING **JUNE 2015**

PAPER 3 MATERIALS (minor corrections made: Feb 2018)

1 (a) (i) Eutectic reaction: 8 wt% Al_2O_3 at 1587 °C, Liquid transforms to Cristoballite and Mullite.
Peritectic reaction: 73 wt% Al_2O_3 at ~1840 °C and ~73 wt% Al_2O_3, Liquid and Alumina transform to Mullite.

(ii) From tie-line through constitution point:
Phases and compositions are: Liquid (~33 wt% Al_2O_3) and Mullite (~71 wt% Al_2O_3).
Proportions of the phases: Liquid (71–50)/(71–33) ≈ 55%; Mullite (50–33)/(71–33) ≈ 45%.

(iii) At 2100 °C, single phase Liquid throughout – *G* falls with composition from both sides, giving a single minimum.

At 1800 °C, there will be 3 *G* curves for Liquid, Mullite and Alumina. In single phase regions, the curve for that phase gives the lowest *G*; in two-phase regions, the curves cross over, and a tangent to both curves gives the total *G* of the two-phase mixture.
From 0 –33 wt%, single phase Liquid has the lowest *G*.
Tangent points to the Liquid and Mullite curves are at the compositions found in (ii) above (33wt% and 71 wt%).
The Mullite curve gives the minimum G over a narrow range, as the first tangent point for the Mullite + Alumina region is at 74 wt%
Alumina has no solubility for SiO_2 – hence the tangent point to the G curve for Alumina must be at the composition 100 wt% Al_2O_3 (or else a single phase Al_2O_3 region would form over a range of composition).

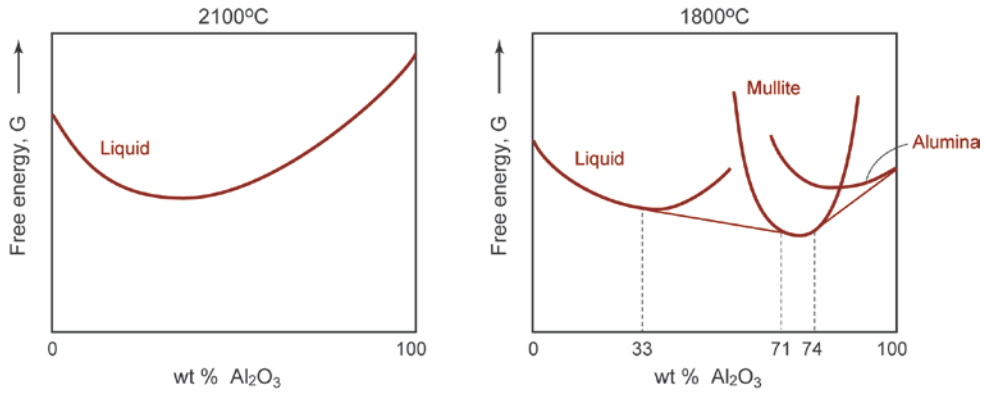

(b) (i) At 1750 °C the equilibrium phase is just Mullite. The micrograph shows a mixture of 3 phases (Alumina, a glassy phase and Mullite). Hence the sample has clearly not reached equilibrium. (At room temperature in this system, only one or two phases can exist at equilibrium – and all the phases are crystalline: the presence of an amorphous glassy phase is in itself an indication that this is not at equilibrium).

On cooling Liquid of composition 73 wt% Al_2O_3, pure Alumina nucleates first (on entering the Al_2O_3 + Liquid field). As the peritectic temperature is approached, the microstructure is a mixture of Alumina plus Liquid with a composition well below that of Mullite (around 55 wt%).

As 30 days has not produced an equilibrium structure of 100% Mullite, this suggests that the peritectic reaction is difficult to nucleate, and requires considerable redistribution of the elements. So we can assume that the primary Alumina remains largely unaffected, so on further cooling to 1750 °C, the Liquid (of composition around 55 wt%) enters the Liquid + Mullite region, leading to the Mullite seen in the micrograph (probably by nucleation on the existing Alumina). This does not consume all of the Liquid – which solidifies on rapid cooling but is unable to crystallise into Cristobalite+Mullite, forming an amorphous glassy phase instead.

(ii) The problem is the very slow diffusion required to enable the Alumina and Liquid to react and form Mullite. One way to enable Mullite formation would be to cool the Liquid rapidly to below the peritectic temperature, so that little or no primary Alumina forms. To form a single crystal of Mullite, we then use a seed crystal of this phase (and at the same time overcome any barrier to nucleation of Mullite from the Liquid).

[*Examiner's comments:* popular question, with average marks. Parts (a, i and ii) were well-answered; (a, iii) was deliberately challenging, for the 1800°C case. In Part (b,i) most candidates identified that the system was not at equilibrium, either because the phase diagram predicts 100% mullite or due to the existence of a glass phase, but the description of the microstructure evolution was very variable, with few pointing out that the glass phase and alumina needed to react, which could be very slow. Very few candidates made a good attempt at (b,ii).]

2. (a) (i) Microstructure of slow-cooled 0.4% C steel:

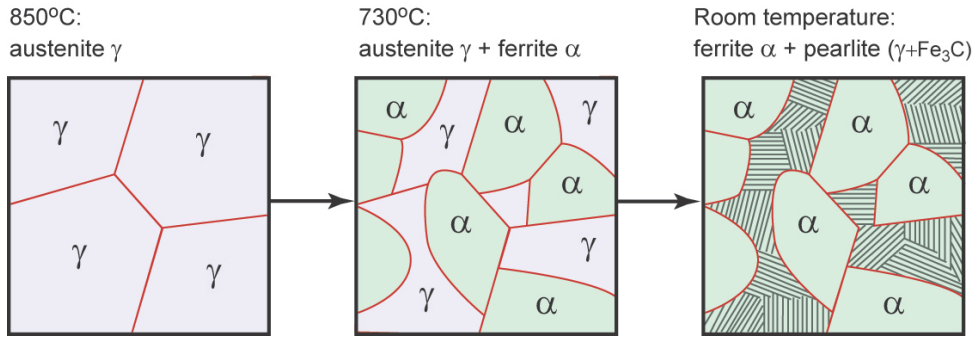

(ii) Microstructure of rapidly cooled 0.4% C steel: martensite

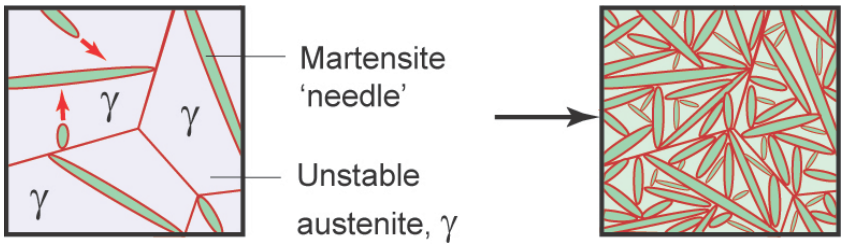

Insufficient time for carbon to diffuse out of the austenite to form iron carbide, but FCC austenite still transforms to BCC lattice by a diffusionless shear transformation to martensite. Needles of martensite nucleate on austenite grain boundaries and traverse grains at speed of sound. Carbon remains trapped in supersaturated solid solution, distorting the BCC lattice.

(b) Hardenability of a steel is the extent to which it can form martensite on cooling, i.e. a hardenable steel forms martensite even with slow cooling. It is measured by the size of component (e.g. bar diameter) that forms a high % of martensite – indicated by the extent to which the hardness remains high (associated with martensite).

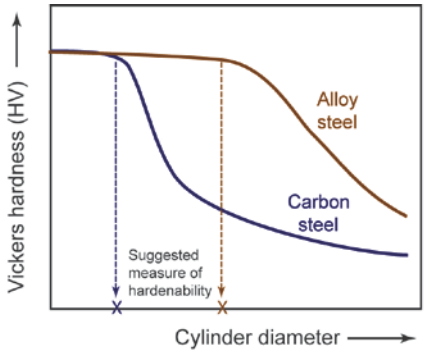

Alloying increases the hardenability of steels by impeding the transformation of FCC austenite to BCC ferrite. The alloying additions form substitutional solid solutions, with different solubility in FCC and BCC iron. Hence they must redistribute to enable the formation of ferrite, which is inherently slow for substitutional elements. Hence more time available (i.e. slower cooling rate) to avoid forming ferrite/pearlite, giving higher hardenability. Typical elements: Ni, Cr, Mo.

(c) (i) Martensite is very brittle; tempering restores the toughness to an acceptable level (while reducing the hardness). The steel is reheated to an intermediate temperature, enabling the carbon to diffuse out and form iron (or alloy) carbides.

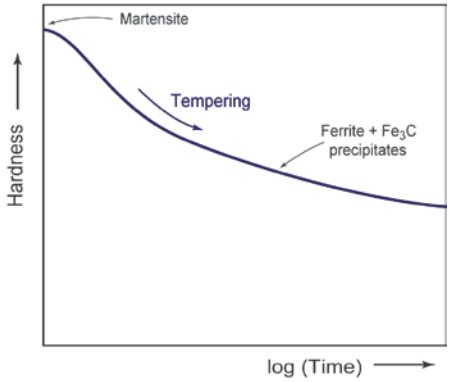

(ii) Similarities between age hardening Al and quench/temper of steels (any two):
- solution heat treatment to take alloying additions into solid solution
- quench to retain supersaturated solid solution
- final strength from precipitation hardening

Diffferences between age hardening Al alloys and quench/temper of steels (any two):
- no FCC-BCC martensitic transformation in Al alloys
- precipitation through sequence of metastable phases in Al alloys (straight to equilibrium carbide in steel)
- ageing curve in Al alloys resulting from transition between dislocations shearing and bypassing precipitates; hardness falls in tempering as precipitates form and coarsen.

[*Examiner's comments:* Very popular and mostly well-answered question. The majority of candidates produced a rather poor diagram for (a,ii) that was not labelled. Marks were lost in (b) by candidates who simply did not read the question and failed to indicate the measure of hardenability on the graph, or plotted low alloy and carbon steel on different axes, such that the difference was not clear. Part (c,ii) produced some vague answers, with candidates writing general points on Al ageing, rather than identifying similarities and differences as requested.]

3. (a) (i) Key difference is the hysteretic behaviour of viscoelastic material, giving a stress-strain loop. Elastic response is linear with negligible hysteresis.

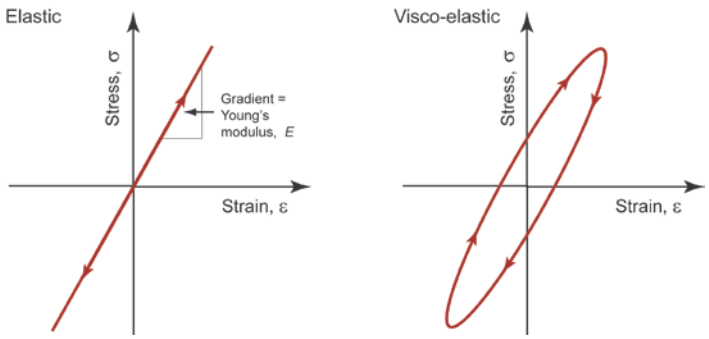

(ii) Real and imaginary components of Young's modulus as function of temperature:

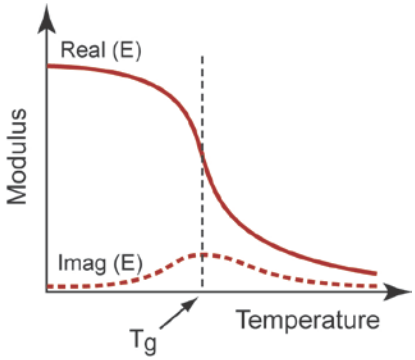

The key observation is that the glass transition temperature T_g corresponds to the peak in the imaginary component of E (maximum energy dissipation); also where the real modulus drops significantly.

(b)

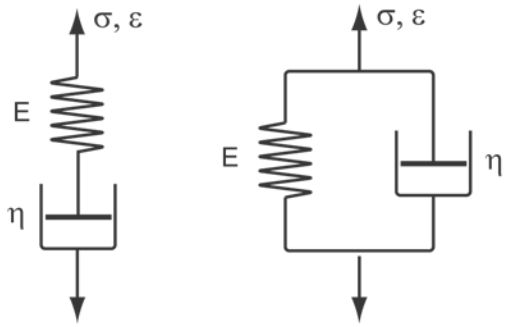

LH (series) case: $\dot{\varepsilon} = \dfrac{\dot{\sigma}}{E} + \dfrac{\sigma}{\eta}$

RH (parallel) case: $\sigma = E\,\varepsilon + \eta\,\dot{\varepsilon}$

(Since the course in IB commonly used *F* and x for σ and ε – both accepted if correct.)

Responses to step in stress:

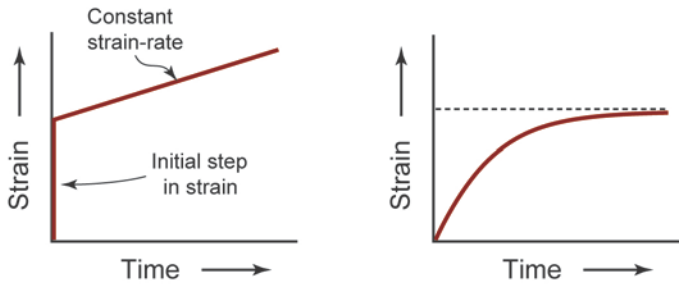

(c) (i)

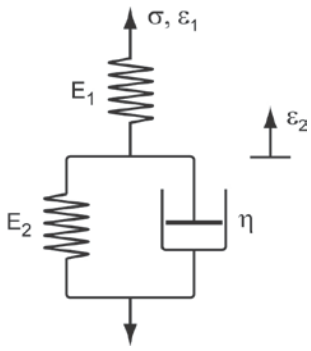

Lower block: $\sigma = E_2\,\varepsilon_2 + \eta\,\dot{\varepsilon}_2$

Upper block: $\sigma = E_1\,(\varepsilon_1 - \varepsilon_2)$

Same stress in both, and $\dot{\sigma} = E_1\,(\dot{\varepsilon}_1 - \dot{\varepsilon}_2)$

Eliminating ε_2 and $\dot{\varepsilon}_2$:

$$\sigma = E_2\left(\varepsilon_1 - \frac{\sigma}{E_1}\right) + \eta\left(\dot{\varepsilon}_1 - \frac{\dot{\sigma}}{E_1}\right)$$

Hence: $\eta\,\dot{\sigma} + (E_1 + E_2)\sigma = E_1\,E_2\,\varepsilon_1 + \eta\,E_1\,\dot{\varepsilon}_1$

With step in stress, dashpot "locks up" and only E_1 strains; subsequent additional strain in only E_2 as dashpot moves.

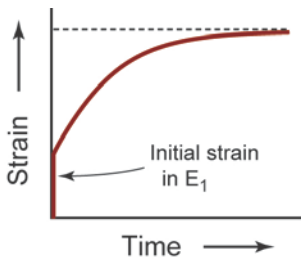

(ii) For high frequency, dashpot locked so only the E_1 spring operates. For low frequency, we can ignore the dashpot so the response is E_1 and E_2 springs in series.

[*Examiner's comments:* Least popular question, but with average marks. In part (a,i) marks were lost by students who sketched stress/strain vs time rather than a stress-strain response as requested. Parts (b,c) were mostly well-answered, though some students (presumably thinking of the 'electrical analogy'), provided the complex moduli of the systems, rather than the governing differential equations requested. Part (c,ii), somewhat surprisingly, produced a large number of vague answers.]

4. (a) (i) The Jominy end-quench is designed to give a continuous variation of cooling rate with distance along a bar made of steel, which is initially in the austenitic state. This gives the full range of metallurgical responses from slow cooling to a rapid quench, as in a CCT diagram. The hardness profile along the bar is therefore an indicator of hardenability of the steel.

(ii) $$\frac{T(x,t)-T_0}{T_1-T_0} = \text{erf}\left(\frac{x}{2\sqrt{at}}\right) \approx \left(\frac{x}{2\sqrt{at}}\right) \quad \left(\text{for } \left(\frac{x}{2\sqrt{at}}\right) < 0.7\right)$$

Inverting the equation: $$t \approx \left(\frac{x^2}{4a}\right)\left(\frac{T_1-T_0}{T-T_0}\right)^2$$

This is valid for X < 0.7, and hence for $\frac{T(x,t)-T_0}{T_1-T_0} < 0.7$

For T_1 = 1000 °C and T_0 = 20 °C, the upper limit on T is therefore (20 + 980×0.7) = 706 °C, and the solution is valid down to 20 °C.

(iii) Time taken between 700 and 400°C given by $t_{400} - t_{700}$:

$$t_{400} - t_{700} \approx \left(\frac{x^2}{4a}\right)\left[\left(\frac{980}{380}\right)^2 - \left(\frac{980}{680}\right)^2\right] \approx 1.143\left(\frac{x^2}{a}\right)$$

Hence the average cooling rate between 700 and 400°C is: $300/(t_{400} - t_{700}) \approx 262\left(\frac{a}{x^2}\right)$

(iv) Inverting the solution for the plate:

$$t = \frac{(2w)^2}{\pi^2 a}\ln\left(\frac{4}{\pi}\frac{T_1-T_0}{T-T_0}\right)$$

Hence

$$t_{400} - t_{700} \approx \left(\frac{(2w)^2}{\pi^2 a}\right)\left[\ln\left(\frac{980}{380}\right) - \ln\left(\frac{980}{680}\right)\right] \approx \left(\frac{(2w)^2}{\pi^2 a}\right)\left[\ln\left(\frac{680}{380}\right)\right] \approx 0.059\left(\frac{(2w)^2}{a}\right)$$

and the average cooling rate between 700 and 400°C is: $300/(t_{400} - t_{700}) \approx 5088\left(\frac{a}{(2w)^2}\right)$

Equating the cooling rates: $262\left(\frac{a}{x^2}\right) = 5088\left(\frac{a}{(2w)^2}\right)$, so relationship between plate thickness (2w) and Jominy distance X_J is: $(2w) \approx 4.40\ X_J$

(b) Two possible processes covered in lectures: carburising of steels, or pre-deposition stage in semiconductor doping.

Carburising is to increase the carbon content near the surface of the steel to increase its hardness and wear resistance (often combined with subsequent surface transformation hardening, to produce high carbon martensite at the surface).

Pre-deposition in semiconductor doping is to deposit a controlled amount of dopant into a near-surface zone in silicon, prior to the drive-in stage which redistributes the dopant to a more uniform level over a much greater depth.

Boundary conditions:
For both processes, surface composition maintained at $C_1 = C_s$
For carburising C_0 = initial composition; doping $C_0 = 0$.

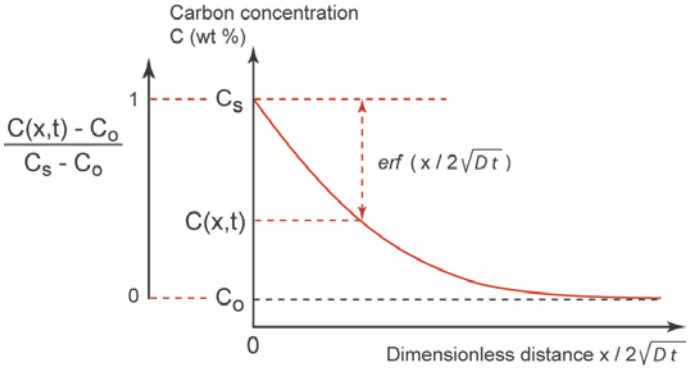

To adapt the heat flow solution, replace temperature T with concentration C, and thermal diffusivity a with diffusion coefficient D.

Solution is upside-down error function, so scale boundary conditions to (erf) as in the figure:

$$\frac{C_s - C(x,t)}{C_s - C_0} = \text{erf}\left(\frac{x}{2\sqrt{Dt}}\right)$$

[*Examiner's comments:* relatively unpopular question, but with average marks and many with complete analysis. The weakest parts, with complete guesswork at times, were invariably the descriptive parts, (a,i) and (b). In the analysis, a number of candidates simply ignored the way cooling rate was defined in the question and tried to differentiate, with limited success.]

5. (a) (i) $\dot{\varepsilon} = A\,\sigma^n \exp(-Q/RT)$

Hence at constant temperature: $\log \dot{\varepsilon} = \log(\text{constant}) + n \log \sigma$

Plot $\log \dot{\varepsilon}$ vs. $\log \sigma$, slope = n

Interpolate log (stress) values (i.e. *linear* interpolation on y-axis) at selected decades of strain-rate, at T = 800°C (points marked on deformation mechanism map below):

Strain-rate (/s)	Log stress (MPa)	Log strain-rate	Mechanism
10^{-10}	– 1	– 10	Diffusional flow
10^{-9}	0	– 9	Diffusional flow
10^{-7}	0.90	– 7	Power-law creep
10^{-4}	1.55	– 4	Power-law creep

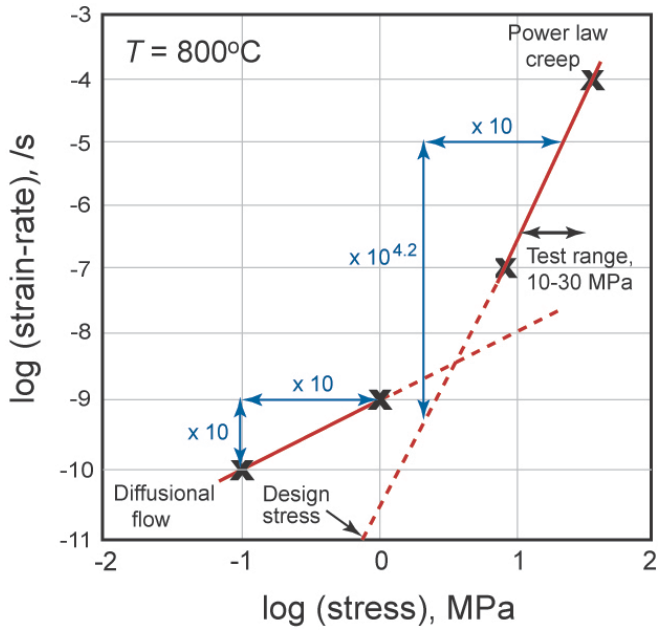

Only 2 values needed per mechanism to estimate slope, as straight line in each case (but more accurate to use more than 2 in power-law creep, where there are more contours).

Easiest to find gradient n by taking one decade in stress, and counting corresponding decades in strain-rate (extrapolating as necessary).

For diffusional flow: $n \approx 1$

For power-law creep: $n \approx 4.2$

(note that the n values sensitive to how the lines are constructed, so any value between 4 and 5 acceptable for power law creep, for example)

(ii) From creep equation, at constant stress: $\ln \dot{\varepsilon} = \ln(\text{constant}) - \dfrac{Q}{RT}$

So read off data at a constant stress within a given mechanism, and construct a conventional Arrhenius plot of $\ln \dot{\varepsilon}$ vs. 1/T. The gradient will be $-Q/R$.

(iii) Test range of stress 10-30 MPa lies within power-law creep regime (see graph above, or mechanism map).
Log (design stress) = log (0.8) MPa = – 0.10
From graph, extrapolating power-law creep gradient to this stress gives a strain rate $\approx 10^{-11}$ /s.

The actual strain-rate at the design stress $\approx 10^{-9.1}$ /s, due to the change in mechanism to diffusional flow – a factor of about 80 times higher than predicted by the tests (and thus unsafe in design).

An acceptable solution is to accelerate the tests by increasing the strain-rate without changing the deformation mechanism (see map below), i.e. increasing the temperature at the design stress to around 1300°C (at which the strain-rate is expected to be around 10^{-7} /s (approx. 100 times faster than at the service temperature).

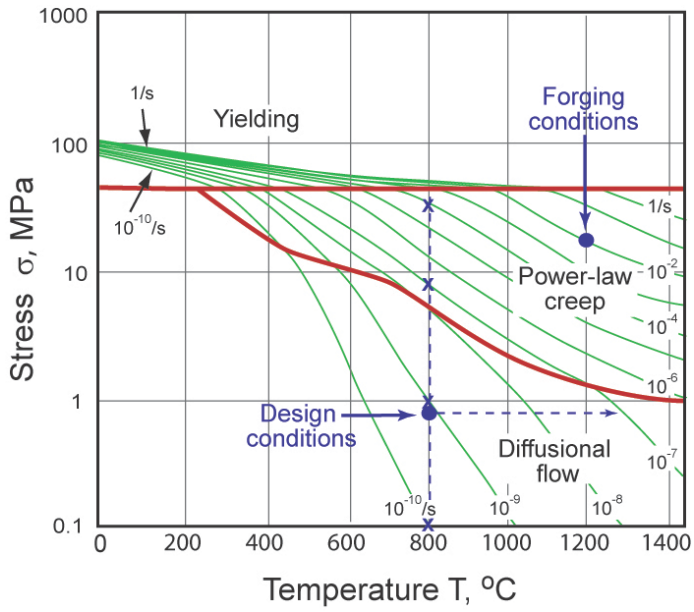

(iv) The initial strain-rate during forging is given by v/h, where v is the speed of the platen, and h is the height of the billet (since $v = dx/dt$, and dx/h is the true strain increment in time dt).

Hence $\dot{\varepsilon} = 1/100\ \text{s}^{-1} = 10^{-2}\ \text{s}^{-1}$.

From mechanism map, at this strain-rate and T = 1200°C, log(stress) ≈ 1.25

Forging stress ≈ 18 MPa.

In practice, the forging stress is likely to be higher because of *friction* – the average pressure in hot forging is higher than the uniaxial yield stress (due to the 'friction hill').

(A more subtle point is that the aspect ratio of the billet will change, increasing the cross-sectional area and further increasing the required stress to hot form the billet – though to counter this effect, the strain-rate will also decrease as the platen decelerates).

(b) Ni-based superalloys for jet engine turbine blades:

High alloy content (e.g. Co, W, Cr, Al, Ti) to give solid solution and precipitation hardening, impeding dislocation mechanism (and thus reducing the rate of power-law creep).

Processing by casting using a 'pigtail' and controlled directional solidification gives a single crystal with no grain boundaries, thus reducing the rate of diffusional flow.

Thermal barrier coatings (e.g. zirconia) may also be used, to reduce the working temperature of the blade (reducing creep-rate of both mechanisms).

[*Examiner's comments:* Relatively unpopular question, with marks a little below average – mainly due to incomplete answers from many candidates doing this question last. Many very good answers to all parts of the question, though rarely all from an individual candidate. In (a,i) many plugged numbers into calculators without showing working or plotting a graph, and were penalised accordingly. Many proposed the use of a y-intercept to find Q/R, assuming incorrectly that the constant A was known – instead of proposing multiple temperatures, and a conventional Arrhenius plot of rate vs. 1/T.]

6. (a) (i) Change in total free energy ΔG_{tot}, for sphere of radius r :

$$\Delta G_{tot} = \frac{4}{3}\pi r^3 (\Delta G) + 4\pi r^2 (\gamma)$$

First term = volume contribution, with change in free energy per unit volume ΔG (negative) being the thermodynamic 'driving force' for liquid to transform to solid (below the equilibrium temperature).

Second term = surface contribution, with the surface energy per unit area γ (positive) being the energy penalty for creating new interface between the liquid and solid phases.

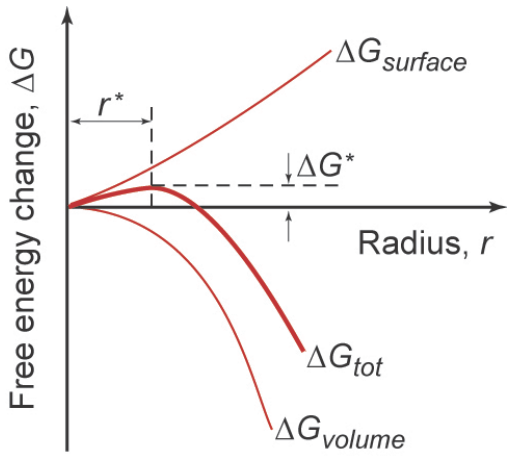

The trade-off between surface term and volume terms leads to a maximum in ΔG_{tot}.

At small radii the surface penalty > volumetric free energy release, so ΔG_{tot} rises.

At large radii, the surface penalty becomes << volumetric term.

The critical radius, r^*, corresponds to the maximum in free energy, ΔG^*, since this is the radius at which (on average) nuclei become stable.

(ii) In practical casting, heterogeneous nucleation is likely to occur from the mould walls, or from solid particles within the melt (impurities, or deliberately added 'inoculants'). The undercooling to reach a stable nucleus is much smaller on another solid surface.

The microstructural characteristic most affected by nucleation in casting is the grain size – each solid nucleus leads to the formation of a grain.

(b) The nucleation process in recrystallization is the formation of subgrains by recovery – dislocations re-arrange into low-angle boundaries. A small number of subgrains then grow, by atomic diffusion across the boundaries between of the new grain and the surrounding deformed material. The driving force is the difference in free energy due to the high dislocation density in the deformed material.

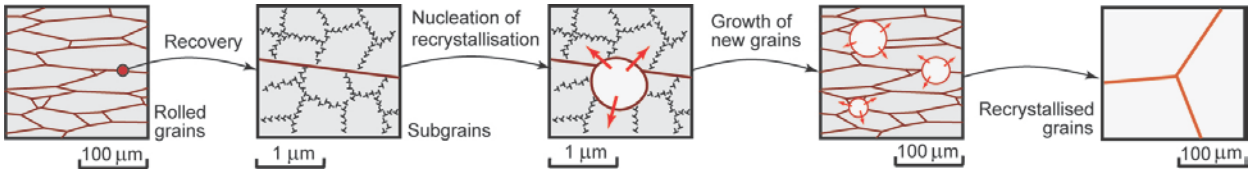

(c) (i) Overall transformation rate depends on two competing temperature-dependent terms:

- ΔG, the thermodynamic driving force, approx. proportional to ΔT (the undercooling)
- $\exp(-Q/RT)$, the kinetic rate of diffusion (Arrhenius law), steeply rising with temperature

Close to the equilibrium temperature, the driving force tends to zero; close to 0 K the diffusion rate tends to zero. The maximum transformation rate occurs at an intermediate temperature, and the maximum rate corresponds to a minimum time to reach every stage in transformation, from 0 to 100% transformed.

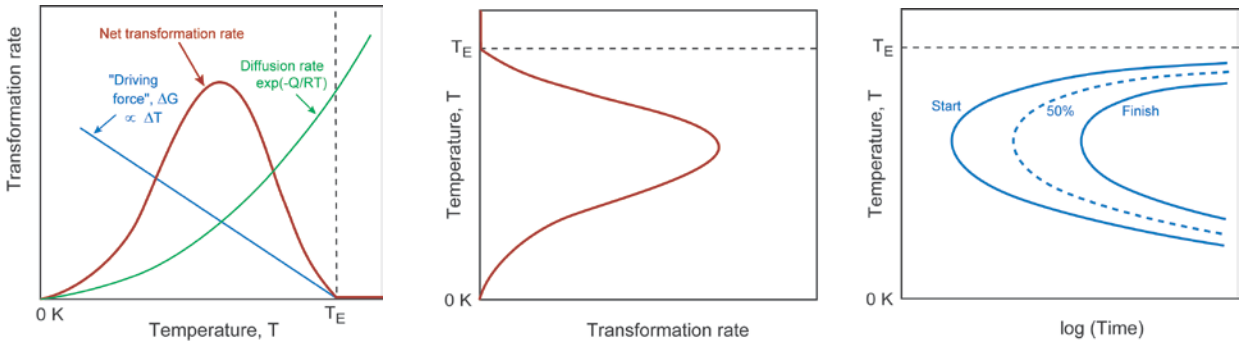

(ii) On heating, the driving force will again be proportional to ΔT, but this increases with temperature *above* T_E. So both the thermodynamic and the kinetic temperature-dependent terms increase on heating above T_E – the transformation rate increases rapidly with temperature, so C-curves are not expected.
(A more subtle point is that there will still be a nucleation barrier, as there is still a surface energy penalty when the new phases forms – but this is more easily overcome on heating).

(iii) Semi-crystalline thermoplastics can crystallise on cooling – the extent of crystallisation is dependent on temperature and time, giving a conventional TTT diagram.

Above the melting temperature (T_m) the amorphous state of the polymer is stable: it is a viscous liquid with randomly orientated molecules.

Below T_m, the difference in free energy between the amorphous and crystalline states provides a *driving force* for crystallisation increasing with undercooling ($T_m - T$).

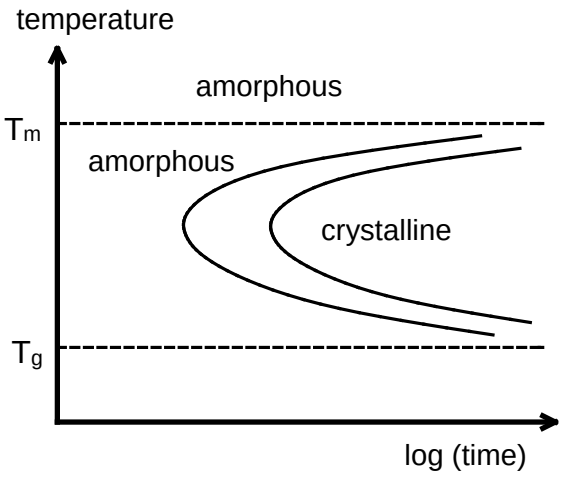

The crystallisation process is also governed by the diffusion *kinetics* of rearranging the polymer chains into crystallites. Below the glass transition temperature (T_g), the van der Waals bonds become stronger, and chain mobility is inhibited, restricting further crystallisation.

[*Examiner's comments:* Popular question, with marks a little below average. In (b) many students gave examples that were nothing to do with casting. The main misconception was in (c,i), that thermodynamics controls nucleation at low undercooling, while kinetics controls growth at large undercooling, whereas ΔG and $\exp(-Q/RT)$ control both nucleation and growth.]

H.R. Shercliff
J.H. Durrell